Research Letter **DOI:** 10.15541/jim20240497

Influence of Cr^{3+} Doping Concentration on the Persistent Performance of YAGG:Ce^{3+},Cr^{3+} Luminescent Ceramics

LI Tingsong[1,2], WANG Wenli[1,3], LIU Qiang[3], WANG Yanbin[1,2], ZHOU Zhenzhen[1,2], HU Chen[1,2], LI Jiang[1,2]

(1. Transparent Ceramics Research Center, Shanghai Institute of Ceramics, Chinese Academy of Sciences, Shanghai 201899, China; 2. Center of Materials Science and Optoelectronics Engineering, University of Chinese Academy of Sciences, Beijing 100049, China; 3. School of Material Science and Engineering, Jiangsu University, Zhenjiang 212013, China)

Abstract: $Y_3Al_2Ga_3O_{12}$:Ce^{3+},Cr^{3+} (YAGG:Ce^{3+},Cr^{3+}), as a persistent luminescent material, has advantages of high initial luminescence intensity and long persistent time, which is promising in persistent luminescent material applications. At present, YAGG:Ce^{3+},Cr^{3+} powders exhibit good persistent performance, but their persistent performance of ceramics still needs to be further improved to meet the new requirements. In this work, $(Y_{0.998}Ce_{0.002})_3(Al_{1-x}Cr_x)_2Ga_3O_{12}$ ceramics with different Cr^{3+} doping concentrations were prepared by solid-state reaction, including air pre-sintering, hot isostatic pressing (HIP) post-treatment and air annealing, to investigate the effects of Cr^{3+} doping concentration on the microstructure, optical properties and persistent performance of the ceramics. The results showed that as the doping concentration of Cr^{3+} increased from 0.025% to 0.2% (in atom), no significant effect of Cr^{3+} concentration on the morphology of pre-sintered ceramics or HIP post-treatment ceramics was observed, but the in-line transmittance gradually increased while the persistent performance gradually decreased. Among them, YAGG:Ce^{3+},Cr^{3+} ceramics doped with 0.025% Cr^{3+} showed the strongest initial luminescence intensity exceeding 6055 mcd/m^2 and a persistent time of 1030 min after air pre-sintering combined with HIP post-treatment and air annealing. By optimizing the Cr^{3+} doping concentration and the fabrication process, the persistent luminescence (PersL) performance of the YAGG:Ce^{3+},Cr^{3+} ceramics was obviously improved.

Key words: YAGG:Ce^{3+},Cr^{3+} ceramic; Cr^{3+} doping concentration; persistent luminescence; hot isostatic pressing; air annealing

PersL is defined as a luminescence phenomenon observed for several minutes or even hours after removal of the excitation sources[1-7]. The unique phenomenon is probably caused by the mechanism of charge carrier trapping and de-trapping processes in PersL materials[3, 8-13]. Due to the unusual optical properties, PersL materials have been widely applied in the fields of decoration, emergency lighting, optical storage and so on[6, 14-17]. Higher performance and stable properties of PersL materials are required for applications in harsh environments, such as high temperatures and high humidity. Compared with the powders, the PersL transparent ceramics exhibit more stable chemical properties and higher PersL efficiency[17-21]. Due to high transparency, the deep penetration of excitation light in ceramics can excite more emitting centers, leading to higher optical efficiency[22-26].

Since the discovery of excellent $SrAl_2O_4$:Eu^{2+},Dy^{3+} persistent phosphors in 1996, many new persistent phosphors, showing PersL with different colors in the visible region, have been synthesized and rapidly replaced the ZnS-based persistent phosphors in the commercial application[2, 4, 27-28]. Among them, the garnet is one of the most widely studied compounds for the host matrix of persistent phosphors[29-32]. The general formula of the garnet is $A_3B_2C_3O_{12}$, and the A, B and C cations can be partially or even completely replaced by the dopant ions, which gives garnets remarkable flexibility in tuning and optimizing the luminescence properties for specific applications[25, 29, 31, 33]. In addition, almost all

Received date: 2024-11-28; **Revised date:** 2024-12-25; **Published online:** 2025-01-24
Foundation item: National Key R&D Program of China (2023YFB3506600)
Biography: LI Tingsong (1998–), male, Master candidate. E-mail: litingsong@mail.sic.ac.cn
李廷松(1998–), 男, 硕士研究生. E-mail: litingsong@mail.sic.ac.cn
Corresponding author: LI Jiang, professor. E-mail: lijiang@mail.sic.ac.cn
李 江, 研究员. E-mail: lijiang@mail.sic.ac.cn

cations of the garnet are trivalent, and there is no problem of charge mismatch when doped with trivalent rare earth ions and transition metal ions. Moreover, it was found that the trap depth could be tuned by the replacement of Al^{3+} by Ga^{3+} because of the band gap changes with the Ga/Al ratio. In general, compared with PersL powders, the PersL ceramics exhibit higher PersL intensity and longer PersL time because of higher crystallinity, larger grain size, and fewer surface defects[17, 24-25, 34-37]. Recently, $Y_3Al_{5-x}Ga_xO_{12}$:Ce,Cr (x=0, 1, 2, 2.5, 3, 3.5, 4 and 5) PersL ceramics have been studied, and the results showed that the decreasing band gap energy with increasing Ga^{3+} content has a significant impact on the PersL intensity of $Y_3Al_{5-x}Ga_xO_{12}$:Ce,Cr, which exhibited the highest intensity at room temperature for the $Y_3Al_2Ga_3O_{12}$ (YAGG) stoichiometry[29, 38-39]. However, the YAGG:Cr^{3+} PersL material cannot achieve PersL after the excitation by blue light, because the energy of blue light is not enough to promote the electrons of Cr^{3+} to the conduction band, and then no charge carrier trapping and de-trapping process happens[40-41]. In order to solve this problem, Ce^{3+} is usually selected as co-dopant ion to increase the absorption cross-section in the blue light region. For the YAGG:Ce^{3+},Cr^{3+} persistent luminescent material, the electrons of Ce^{3+} can be excited to the conduction band and then captured by the traps. After switching off the excitation source, the captured electrons may return to Ce^{3+}, and then the PersL energy transfer happens from Ce^{3+} to Cr^{3+}, leading to PersL in YAGG:Ce^{3+},Cr^{3+}[41-42]. In addition, compared to luminescent powders, ceramics exhibit higher PersL intensity and longer PersL time. The YAGG:Ce^{3+},Cr^{3+} ceramics with excellent persistent performance can rival commercial $SrAl_2O_4$ ceramics and are used in safety signage applications, such as emergency exit signs in buildings and guiding strips in aisles of airplanes[38].

Increasing the concentration of the emitting centers is an effective way to improve the luminescence intensity. However, when the concentration of the emitting centers is too high, luminescence quenching (or concentration quenching) may occur due to the interactions between the emitting centers, such as excited state absorption and cross relaxation[42]. The excitation energy may be transferred from one emitting center to another and eventually to an imperfection which may work as an energy sink, leading to nonradiative transition and reduced luminescence intensity[43-45]. For the YAGG:Ce^{3+},Cr^{3+} PersL ceramics, the influence of Ce^{3+} concentration on the luminescence intensity has already been investigated. The results indicate that luminescence quenching occurs when the Ce^{3+} concentration exceeds 0.2%[26]. In order to obtain the optimal concentration of Cr^{3+} to improve the luminescence intensity, the effect of Cr^{3+} concentration on the optical properties of the YAGG:Ce^{3+},Cr^{3+} PersL ceramics was also systematically investigated.

In this work, the YAGG:Ce^{3+},Cr^{3+} PersL ceramics containing different concentrations of Cr^{3+}, were fabricated by solid-state reaction method. The influences of Cr^{3+} concentration on the crystalline structure, micro-morphology and optical transmittance of YAGG:Ce^{3+},Cr^{3+} PersL ceramics were investigated, and the effect of Cr^{3+} concentration on the PersL intensity was also studied. The results showed that when the Cr^{3+} concentration was 0.025% (in atom), the ceramics exhibited the strongest PersL intensity. With a further increase of Cr^{3+} amount, the PersL intensity showed a slight reduction due to energy transfer from Ce^{3+} to Cr^{3+}.

1 Experimental

Commercial powders of Y_2O_3 (Shanghai Sinian Metal Materials Co., Ltd., 99.999%), Ga_2O_3 (Shandong Jining Zhongkai New Materials Co., Ltd., 99.995%), α-Al_2O_3 (Hangzhou Zhongtianli New Materials Co., Ltd., 99.99%), CeO_2 (Fujian Changting Jinlong Rare Earth Co., Ltd., 99.99%) and Cr_2O_3 (Xiamen Jiuyao Tongchuang New Materials Co., Ltd., 99.99%) were used as raw materials. The $(Y_{0.998}Ce_{0.002})_3(Al_{1-x}Cr_x)_2Ga_3O_{12}$ (x=0.025%, 0.05%, 0.1%, 0.2%, in atom) PersL ceramics, indexed as YAGG:Ce^{3+},Cr^{3+} below, were fabricated by the solid-state reaction method, and more detailed information can be found in the previous work[26]. The green body was pre-sintered at 1650 ℃ for 20 h in air followed by HIP post-treatment at 1550 ℃ for 3 h under 176 MPa in Ar. The YAGG:Ce^{3+},Cr^{3+} PersL ceramics were annealed at 1250 ℃ for 5 h in air and then polished on two sides (2.1 mm in thickness) for further characterization.

The crystalline structure of the samples was analyzed by X-ray diffraction (XRD) method (Cu Kα1 radiation, λ=0.15405 nm, Bruker D8 Focus). The field emission scanning electron microscopy (FESEM, Hitachi SU8220) images were acquired to study the surface morphology of the YAGG:Ce^{3+},Cr^{3+} PersL ceramics. The in-line transmittance of the ceramics was measured by a Cary 5000 UV-VIS-NIR spectrophotometer (Varian Inc., USA). The photoluminescence (PL) spectra were recorded by a fluorescence spectrophotometer (F-4600, Hitachi, Japan). PersL properties including PersL initial intensity and duration were recorded by a PR-305 PersL tester (SanSe, Zhejiang, China) after irradiation by a 365 nm UV lamp (24 W) for 5 min.

2 Results and discussion

Fig. 1 shows XRD patterns of pre-sintered combined with HIP post-treated YAGG:Ce^{3+},Cr^{3+} PersL ceramics with different Cr^{3+} concentrations. XRD patterns are in good agreement with $Y_3Al_2Ga_3O_{12}$ crystalline phase (YAGG, PDF#89-6660), indicating that the pure cubic YAGG phase is successfully obtained. No additional diffraction peaks are easily observed with increasing Cr^{3+} concentration. The influence of dopant ions on the crystalline structure of the ceramics cannot be observed with the XRD setup used because of the low concentration of Cr^{3+}.

Fig. 2 shows the surface FESEM images of pre-sintered YAGG:Ce^{3+},Cr^{3+} PersL ceramics with different Cr^{3+} concentrations. No significant influence of Cr^{3+} concentration on the morphology of the ceramics can be observed in the FESEM images with increasing Cr^{3+} concentration. Lots of residual micro-pores, including inter- and intra-crystalline micro-pores, can be easily found. The residual micro-pores are mainly caused by the low pre-sintering temperature. Usually, for the powders prepared by the ball-milling method, vacuum sintering and high sintering temperature are required to remove the micro-pores and obtain the high-density ceramics, due to the large particle size and low sintering ability of the powders. However, when the YAGG:Ce^{3+},Cr^{3+} PersL ceramics are vacuum-sintered at high temperature, the gallium may volatilize from the ceramics, leading to the formation of Ga^{3+} vacancy. Special post-treatments, such as HIP, are needed to remove micro-pores and obtain high-density YAGG:Ce^{3+},Cr^{3+} PersL ceramics at relatively low temperatures in order to avoid the volatilization of gallium.

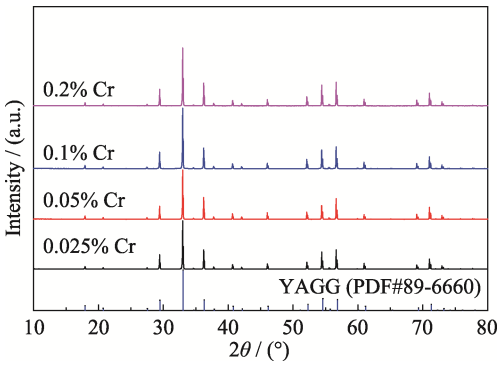

Fig. 1　XRD patterns of pre-sintered combined with HIP post-treated YAGG:Ce^{3+},Cr^{3+} PersL ceramics with different concentrations of Cr^{3+}

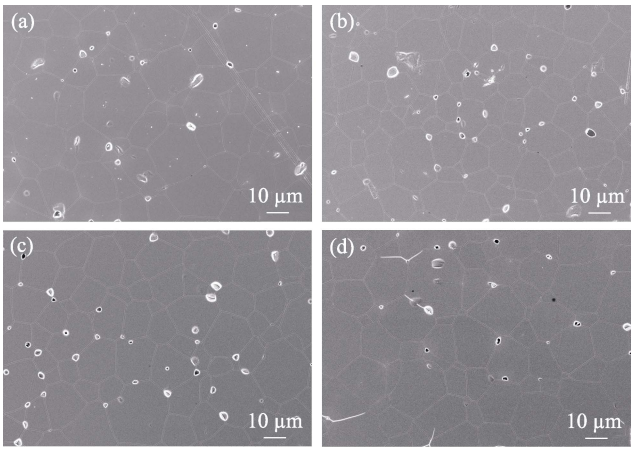

Fig. 2　FESEM images of pre-sintered YAGG:Ce^{3+},Cr^{3+} PersL ceramics with different concentrations of Cr^{3+}
(a) 0.025%; (b) 0.05%; (c) 0.1%; (d) 0.2%

Fig. 3 shows the surface FESEM images of HIP post-treated YAGG:Ce^{3+},Cr^{3+} PersL ceramics with different Cr^{3+} concentrations. In comparison with the FESEM images in Fig. 2, fewer micro-pores can be found in Fig. 3. During the HIP post-treatment, some micro-pores are driven out from the ceramics with the assistance of high pressure through the argon, and then the ceramics with higher density are obtained. However, some intra-crystalline micro-pores are difficult to remove from ceramics, even under high pressure. At times, some open pores can also be easily observed in the FESEM images. These micro-pores remain in the ceramics and work as scattering centers to lower the in-line transmittance. The transmittance test of ceramics also shows a low transmittance, which is consistent with the FESEM morphology results.

Fig. 4 presents the photographs (the Cr^{3+} doping concentrations from left to right are 0.025%, 0.05%, 0.1%, and 0.2%, respectively) and in-line transmittance of YAGG:Ce^{3+},Cr^{3+} PersL ceramics (2.1 mm in thickness) after HIP post-treatment. As shown in Fig. 4(a), the green color of the ceramics is probably caused by the strong absorption in the blue light region of Ce^{3+}. The text behind the ceramics can be observed, while some of them look slightly cloudy, indicating the presence of lots

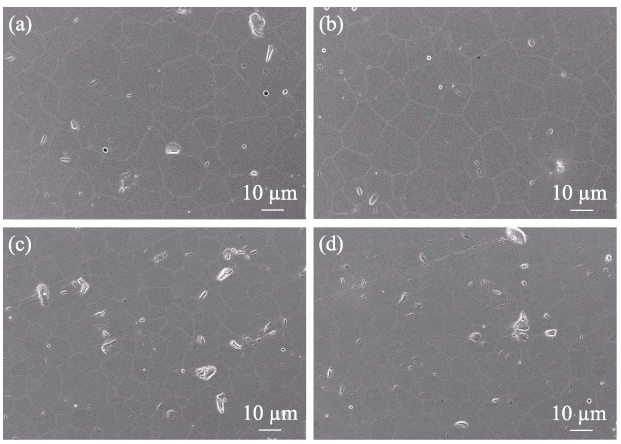

Fig. 3　FESEM images of HIP post-treated YAGG:Ce^{3+},Cr^{3+} PersL ceramics with different concentrations of Cr^{3+}
(a) 0.025%; (b) 0.05%; (c) 0.1%; (d) 0.2%

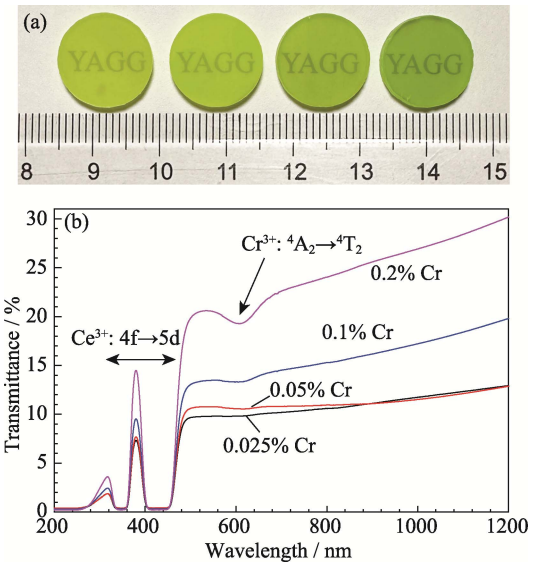

Fig. 4 Photographs and in-line transmittance of pre-sintered combined with HIP post-treated YAGG:Ce^{3+},Cr^{3+} PersL ceramics with different concentrations of Cr^{3+} (2.1 mm in thickness)
(a) Photographs of ceramics (from left to right containing 0.025%, 0.05%, 0.1%, and 0.2% Cr, respectively); (b) In-line transmittance of ceramics

of scattering centers, such as micro-pores. The in-line transmittances (Fig. 4(b)) of the YAGG:Ce^{3+},Cr^{3+} PersL ceramics are 12.9%, 12.9%, 19.8% and 30.2% at 1200 nm when doped with Cr^{3+} concentrations of 0.025%, 0.05%, 0.1%, and 0.2%, respectively. The low in-line transmittance is mainly related to the residual micro-pores, which can be clearly found in FESEM images of Fig. 3. The result indicates that doping Cr^{3+} can improve the optical quality of the YAGG:Ce^{3+},Cr^{3+} PersL ceramics, and Cr^{3+} may act as a sintering aid to improve the in-line transmittance of ceramics. Two broad absorption bands are observed at about 430 and 345 nm due to the transitions from 4f level to the lowest $5d^1$ and second lowest $5d^2$ levels of Ce^{3+} ions, respectively. Besides, an additional broad band at about 606 nm appears in the Cr^{3+} co-doped specimen, which is ascribed to the transition from $^4A_2$ to $^4T_2$ of Cr^{3+}. And as the concentration of Cr^{3+} increases from 0.025% to 0.2%, absorption becomes more pronounced.

Fig. 5(a) shows the PL spectra of pre-sintered combined with HIP post-treated YAGG:Ce^{3+},Cr^{3+} PersL ceramics with different Cr^{3+} concentrations at room temperature, under the excitation of 405 nm. In the PL spectra, the transitions of the Ce^{3+}: $5d^1 \rightarrow 4f^1$ (band centered at 508 nm), Cr^{3+}: $^4T_{2g} \rightarrow {}^4A_{2g}$ (band centered at 707 nm) and ^2E_g,$^2T_{1g} \rightarrow {}^4A_{2g}$ (*R* lines at about 690 nm) were detected in visible light range. The PL intensity originating from Ce^{3+} ions of ceramics gradually decreased, and the PL intensity originating from Cr^{3+} ions gradually increased with increasing Cr^{3+} concentration. As the concentration of Cr^{3+} increases, the emission intensity of Ce^{3+} decreases due to increased energy transfer from Ce^{3+} to Cr^{3+}. The gradual increase in Cr^{3+} transition at 707 nm also confirms this. Thermal stability is one of the key properties for the application of PersL materials in emergency indicator lighting. Fig. 5(b) shows the temperature-dependent PL spectra of ceramics with the Cr^{3+} concentration of 0.025%. Under 405 nm violet excitation, the emission band of the ceramics appears in the range of 450–625 nm with a peak around 508 nm. The phonon assisted non-radiative transitions increase with increasing temperature. When the temperature increases from 300 to 500 K, the luminous intensity of the ceramics can still retain 50% of that at room temperature.

The PersL photographs of YAGG:Ce^{3+},Cr^{3+} PersL ceramics with different Cr^{3+} concentrations pre-sintered at 1650 ℃ for 20 h in air (Fig. 6(a)), HIP post-treated at 1550 ℃ for 3 h under 176 MPa in Ar (Fig. 6(b)) and annealed at 1250 ℃ for 5 h in air (Fig. 6(c)) were taken at different times after the removal of UV excitation source (365 nm). The bright green PersL of all ceramics can be observed at 5 min after switching off the excitation source. At 60 and 120 min, the intensities of

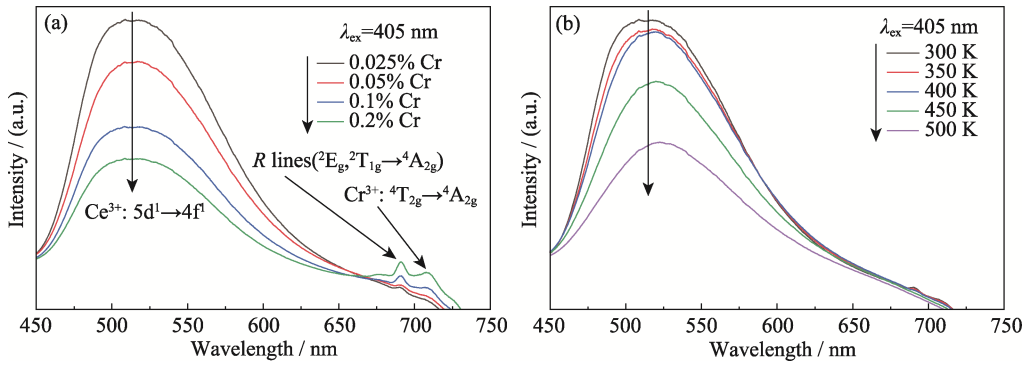

Fig. 5 PL spectra of pre-sintered combined with HIP post-treated YAGG:Ce^{3+},Cr^{3+} PersL ceramics
(a) PL spectra of ceramics with different Cr^{3+} doping concentrations at room temperature; (b) Temperature-dependent PL spectra of ceramics with Cr^{3+} concentration of 0.025%

PersL become weaker, but can still be detected by camera, which indicates that the PersL duration of all ceramic samples is longer than 2 h, proving the promising potential application of YAGG:Ce^{3+},Cr^{3+} PersL ceramics. Figs. 6(d, e) show the initial luminescence intensity and duration of pre-sintered, HIP post-treated, and air annealed YAGG:Ce^{3+},Cr^{3+} PersL ceramics with different Cr^{3+} concentrations (excitation: 365 nm, 24 W, 5 min). The influence of Cr^{3+} concentration on the PersL performance (initial intensity and duration) is analyzed and presented. The initial intensity of pre-sintered ceramics shows a monotonical decrease from 5382 mcd/m^2 to 2102 mcd/m^2 with the increase of Cr^{3+} concentration from 0.025% to 0.2%. The PersL duration also exhibits a similar tendency, decreasing from 430 to 226 min. When the doping concentration of Cr^{3+} is 0.025%, pre-sintered ceramics show the strongest initial luminescence intensity and duration. The variations of initial luminescence intensity and duration with Cr^{3+} concentration in HIP post-treated ceramics and air annealed ceramics are similar to those of pre-sintered ceramics. When the Cr^{3+} doping concentration is 0.025%, they all exhibit the maximum initial luminescence intensity and duration. This indicates that within the range of Cr^{3+} doping concentration, 0.025% Cr^{3+} has the best PersL performance. Among them, the ceramics doped with 0.025% Cr^{3+} exhibit the strongest initial luminescence intensity exceeding 6055 mcd/m^2 and the persistent time of 1030 min after air pre-sintering combined with HIP post-treatment and air annealing. The persistent performance of ceramics exceeds this team's previous research work[26]. In addition, previous research results have shown that the Cr^{3+} co-doped specimens exhibit brighter PersL than the Ce^{3+} single doped one[42]. This is because Ce^{3+} ions act as luminescent centers in YAGG, which affect the luminescence intensity of PersL materials, while Cr^{3+} ions act as sensitizers and undergo energy transfer with Ce^{3+} ions to enhance luminescence intensity, greatly prolonging the time for electrons to return from traps to $5d^1$ level and enhancing the duration. However, YAGG:Cr^{3+} can only achieve PersL after the excitation by X-ray excitation. The PersL after 365 nm irradiation differs greatly from such emissions after X-rays[40-41]. Therefore, YAGG:Cr^{3+} cannot achieve PersL after the excitation by 365 nm light, because the energy of 365 nm light is not enough to promote the electrons of Cr^{3+} to the conduction band, resulting in no charge carrier trapping and de-trapping process occurring. From Figs. 6(d, e), it can be seen that with the increase of Cr^{3+} concentration, the initial luminescence intensity and duration of the ceramics prepared under three conditions show a monotonic decreasing trend. Therefore, only an appropriate Cr^{3+} doping concentration can enhance the PersL performance of YAGG:Ce^{3+} PersL ceramics. This indicates that excessive Cr^{3+} does not participate in energy storage (carrier capture) and even reduces the efficiency of carriers trapping[41]. On the other hand, as the concentration of Cr^{3+} decreases, the PersL performance of ceramics significantly decreases, most probably due to low concentration of donor ions. For ceramics prepared with high concentrations of Cr^{3+} doped YAGG:Ce^{3+}, a significant decrease in initial luminescence intensity and duration is detected, which may be due to the energy transfer of Ce^{3+} to excessive Cr^{3+}.

Air annealed ceramics have better initial luminescence intensity, while HIP post-treated ceramics have longer duration. The initial luminescence intensity of ceramics after HIP post-treatment decreases, but the duration is significantly improved compared to the pre-sintered ceramics. Additionally, air annealed ceramics can maintain stronger initial luminescence intensity while ensuring duration. Based on the earlier reports[26, 30-31, 41, 46] and the results obtained in this work, the energy band diagram of YAGG:Ce^{3+},Cr^{3+} PersL ceramics is constructed to illustrate the PersL mechanism in the YAGG:Ce^{3+},Cr^{3+} PersL ceramics (Fig. 7). The energy band diagram for YAGG:Ce^{3+},Cr^{3+} PersL ceramics is composed of relevant parts of the energy level schemes of the Ce^{3+}, Cr^{3+}, as well as the conduction band and valence band with the main trapping levels in the YAGG host materials. It is known that not only Cr but also lattice defects, such as oxygen vacancies, can lead to trap formation. The traps related to oxygen vacancies are deep for the phosphors operating at room temperature, and more thermal stimulation is needed to release the captured electrons from these traps. HIP post-treatment in Ar atmosphere can generate more oxygen vacancies, and some electrons enter the traps formed by oxygen vacancies, resulting in a decrease in the number of electrons entering other traps. Therefore, the initial luminescence intensity of the ceramics decreases, but the duration increases. After air annealing, some oxygen vacancies are eliminated, so more electrons could be captured by the traps with appropriate trap depths, thereby improving the initial luminescence intensity. But the oxygen vacancies that have not been eliminated ensure that the ceramics exhibit good duration. Air pre-sintered ceramics have the fewest oxygen vacancies, which means there are also the fewest defects, resulting in the shortest duration. On the other hand, HIP post-treated ceramics and air annealed ceramics, due to their transparent characteristics, can excite electrons located deeper in the excitation light source, which is

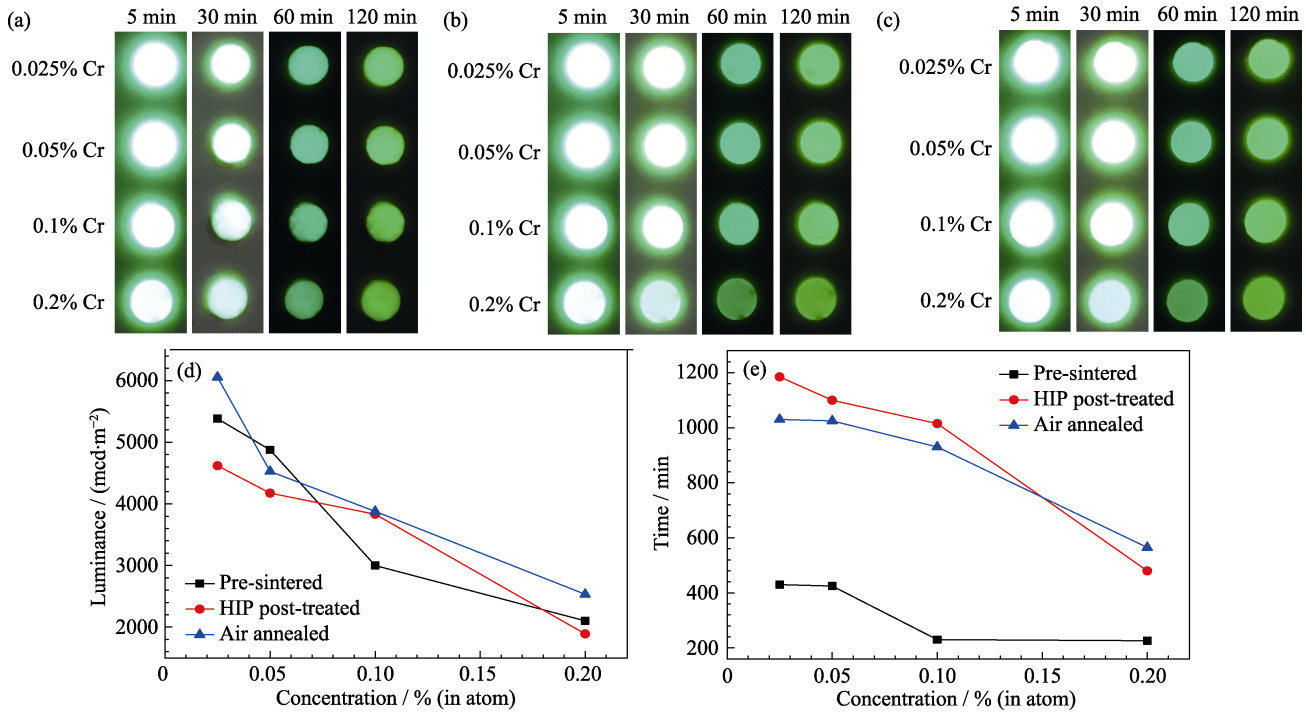

Fig. 6 Luminous photographs, initial luminescence intensity and duration of pre-sintered, HIP post-treated and air annealed YAGG:Ce^{3+},Cr^{3+} PersL ceramics with different concentrations of Cr^{3+} (excitation: 365 nm, 24 W, 5 min)

(a) Luminous photographs of pre-sintered ceramics; (b) Luminous photographs of HIP post-treated ceramics; (c) Luminous photographs of air annealed ceramics; (d) Initial luminescence intensity of ceramics; (e) Duration of ceramics

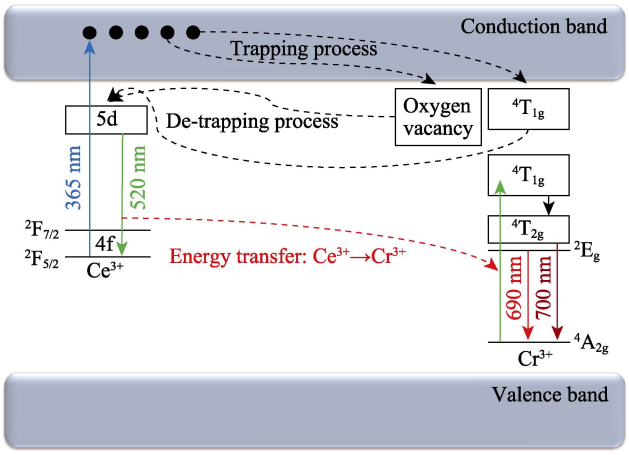

Fig. 7 Energy band diagram of YAGG:Ce^{3+},Cr^{3+} PersL ceramics

equivalent to more electrons participating in the process of PersL. These electrons re-enter the trap and undergo energy transfer with Cr^{3+} ions. The electrons that undergo energy transfer are captured in the trap for a long time and only overflow from the trap and return to the conduction band after another energy transfer with Cr^{3+}. This process greatly slows down the time for electrons to return to the ground state from traps, thus prolonging the duration of persistence.

3 Conclusions

In summary, using the commercial powders of Y_2O_3, Ga_2O_3, α-Al_2O_3, CeO_2 and Cr_2O_3 as raw material, $(Y_{0.998}Ce_{0.002})_3(Al_{1-x}Cr_x)_2Ga_3O_{12}$ (x=0.025%, 0.05%, 0.1%, 0.2%) PersL ceramics were fabricated by air pre-sintering, HIP post-treatment and air annealing. The influences of Cr^{3+} doping on the phase composition, microstructure, optical properties and persistent performance of ceramics were studied. The results showed that when the doping concentration of Cr^{3+} increased from 0.025% to 0.2%, pure cubic YAGG phase was successfully obtained in HIP post-treated ceramics. No significant effect of Cr^{3+} concentration on ceramic morphology was observed in the FESEM images. HIP post-treatment made ceramics denser and reduced porosity. The in-line transmittance of YAGG:Ce^{3+},Cr^{3+} PersL ceramics increased with increasing Cr^{3+} doping concentration. The ceramics with 0.2% Cr^{3+} prepared by HIP post-treatment achieved a linear transmittance of 30.2% at 1200 nm. Under 405 nm violet excitation, the emission band of the ceramics appeared in the range of 450–625 nm with a peak around 508 nm. When the temperature increased from room temperature to 500 K, the luminous intensity of the ceramics could still retain 50% of that at room temperature. As the concentration of Cr^{3+} increased from 0.025% to 0.2%, the initial luminescence intensity of pre-sintered ceramics, HIP post-treated ceramics, and air annealed ceramics gradually decreased. The PersL duration also exhibited a similar tendency. When the Cr^{3+} doping concentration was 0.025%, they all exhibited the

maximum initial luminescence intensity and duration. This indicated that within the range of Cr^{3+} doping concentration, 0.025% Cr^{3+} had the best PersL performance. For all prepared ceramics, the ceramics with the strongest initial luminescence intensity were prepared by doping 0.025% Cr^{3+} and air annealing, with an intensity exceeding 6055 mcd/m^2. The ceramics with the longest duration were prepared by doping 0.025% Cr^{3+} with HIP post-treatment, lasting more than 1185 min. Finally, the influence of oxygen vacancies and ion energy transfer in traps was analyzed. In short, the preparation of YAGG:Ce^{3+},Cr^{3+} PersL ceramics with high PersL intensity and long persistent emission decay time will advance the development and application of PersL materials in the future.

References:

[1] POELMAN D, VAN DER HEGGEN D, DU J, *et al*. Persistent phosphors for the future: fit for the right application. *Journal of Applied Physics*, 2020, **128(24):** 240903.

[2] XU J, TANABE S. Persistent luminescence instead of phosphorescence: history, mechanism, and perspective. *Journal of Luminescence*, 2019, **205:** 581.

[3] LI Y, GECEVICIUSA M, QIU J R. Long persistent phosphors-from fundamentals to applications. *Chemical Society Reviews*, 2016, **45(8):** 2090.

[4] MATSUZAWA T, AOKI Y, TAKEUCHI N, *et al*. A new long phosphorescent phosphor with high brightness, $SrAl_2O_4$:Eu^{2+},Dy^{3+}. *Journal of the Electrochemical Society*, 2019, **143(8):** 2670.

[5] CHERNOV V, SALAS-CASTILLO P, DÍAZ-TORRES L A, *et al*. Thermoluminescence and infrared stimulated luminescence in long persistent monoclinic $SrAl_2O_4$:Eu^{2+},Dy^{3+} and $SrAl_2O_4$:Eu^{2+},Nd^{3+} phosphors. *Optical Materials*, 2019, **92:** 46.

[6] SMET P F, BOTTERMAN J, VAN DEN EECKHOUT K, *et al*. Persistent luminescence in nitride and oxynitride phosphors: a review. *Optical Materials*, 2014, **36(11):** 1913.

[7] XUE H L, YANG M P, SUN J J, *et al*. Study on the flux for $SrAl_2O_4$:Eu^{2+}, Dy^{3+} phosphor preparation used in fluorescent fiber. *Ceramics International*, 2024, **50(1):** 1137.

[8] HÖLSÄ J. Persistent luminescence beats the afterglow: 400 years of persistent luminescence. *Journal of the Electrochemical Society*, 2009, **18(4):** 42.

[9] ZENG Q Q, WU Y Z, CHENG H Y, *et al*. Calcium doped self-activated zinc germanate long afterglow materials: multicolor afterglow and application in dynamic anti-counterfeiting. *Journal of Inorganic Materials*, 2023, **38(8):** 901.

[10] CAI Y Y, LIU S B, ZHAO L, *et al*. Delayed stress memory by $CaAl_2O_4$:Eu^{2+} mechanoluminescent phosphor with defect engineering regulation. *Journal of Advanced Ceramics*, 2022, **11(8):** 1319.

[11] ZHOU S H, LOU B B, MA C G, *et al*. First-principles study on persistent luminescence mechanism of $LiYGeO_4$:Eu^{3+}. *Journal of Rare Earths*, 2023, **41(10):** 1519.

[12] LI Q L, LI N X, LI Y C, *et al*. Research progress of radio-photoluminescence materials and their applications. *Journal of Inorganic Materials*, 2023, **38(7):** 731.

[13] ZHAO J T, LEI L, YE R G, *et al*. Sunlight activated ultra-stable long persistent luminescence glass ceramic for outdoor information display. *Journal of Advanced Ceramics*, 2022, **11(6):** 974.

[14] VAN DEN EECKHOUT K, POELMAN D, SMET P F. Persistent luminescence in non-Eu^{2+}-doped compounds: a review. *Materials*, 2013, **6(7):** 2789.

[15] ZHENG H R, LIU L, LI Y A, *et al*. X-ray excited Mn^{2+}-doped persistent luminescence materials with biological window emission for *in vivo* bioimaging. *Journal of Rare Earths*, 2024, **42(1):** 28.

[16] YIN X G, ZHONG H Y, LIU L, *et al*. X-ray-activated Bi^{3+}/Pr^{3+} co-doped $LiYGeO_4$ phosphor with UV and NIR dual-emissive persistent luminescence. *Journal of Rare Earths*, 2024, **42(5):** 955.

[17] DONG S M, WANG J Y, NI D W. Structural ceramics-the cornerstone of human civilization. *Journal of Inorganic Materials*, 2024, **39(6):** 569.

[18] ZHUANG Y X, KATAYAMA Y, UEDA J, *et al*. A brief review on red to near-infrared persistent luminescence in transition-metal-activated phosphors. *Optical Materials*, 2014, **36(11):** 1907.

[19] KADENGE V, KIPROTICH S, KAWIRA M, *et al*. Effect of Dy^{3+} concentrationson the structural and optical properties of $SrAl_2O_4$:Eu^{2+},Dy^{3+} NPs. *Trends in Sciences*, 2024, **21:** 1.

[20] YANG L, GAI S L, DING H, *et al*. Recent progress in inorganic afterglow materials: mechanisms, persistent luminescent properties, modulating methods, and bioimaging applications. *Advanced Optical Materials*, 2023, **11(11):** 2202382.

[21] LIANG L L, CHEN J Y, SHAO K, *et al*. Controlling persistent luminescence in nanocrystalline phosphors. *Nature Materials*, 2023, **22:** 289.

[22] ZHUANG Y X, UEDA J, TANABE S. Photochromism and white long-lasting persistent luminescence in Bi^{3+}-doped $ZnGa_2O_4$ ceramics. *Optical Materials Express*, 2012, **2(10):** 1378.

[23] ZHUANG Y X, UEDA J, TANABE S. Enhancement of red persistent luminescence in Cr^{3+}-doped $ZnGa_2O_4$ phosphors by Bi_2O_3 codoping. *Applied Physics Express*, 2013, **6(5):** 052602.

[24] DAI Z F, MAO X Y, LIU Q, *et al*. Effect of dopant concentration on the optical characteristics of Cr^{3+}:$ZnGa_2O_4$ transparent ceramics exhibiting persistent luminescence. *Optical Materials*, 2022, **125:** 112127.

[25] DAI Z F, BOIKO V, GRZESZKIEWICZ K, *et al*. Effect of annealing treatment on the persistent luminescence of $Y_3Al_2Ga_3O_{12}$:Ce^{3+}, Cr^{3+},Pr^{3+} ceramics. *Optical Materials*, 2020, **105:** 109888.

[26] LIU Q, WANG W L, DAI Z F, *et al*. Fabrication and long persistent luminescence of Ce^{3+}-Cr^{3+} co-doped yttrium aluminum gallium garnet transparent ceramics. *Journal of Rare Earths*, 2022, **40(11):** 1699.

[27] YANG Y M, LI Z Y, ZHANG J Y, *et al*. X-ray-activated long persistent phosphors featuring strong UVC afterglow emissions. *Light: Science & Applications*, 2018, **7:** 88.

[28] LI T S, LIU Q, ZHU D Y, *et al*. Fabrication and characterizations of Eu^{2+}-Dy^{3+} co-doped $SrAl_2O_4$ ceramics with persistent luminescence. *Journal of the American Ceramic Society*, 2023, **106(10):** 5877.

[29] UEDA J, DORENBOS P, BOS A J J, *et al*. Control of electron transfer between Ce^{3+} and Cr^{3+} in the $Y_3Al_{5-x}Ga_xO_{12}$ host *via* conduction band engineering. *Journal of Materials Chemistry C*, 2015, **3(22):** 5642.

[30] XU J, MURATA D, UEDA J, *et al*. Toward rechargeable persistent luminescence for the first and third biological windows *via* persistent energy transfer and electron trap redistribution. *Inorganic chemistry*, 2018, **57(9):** 5194.

[31] DAI Z F, BOIKO V, GRZESZKIEWICZ K, *et al*. Effect of annealing temperature on persistent luminescence of $Y_3Al_2Ga_3O_{12}$:Cr^{3+} co-doped with Ce^{3+} and Pr^{3+}. *Optical Materials*, 2021, **111:** 110522.

[32] DAI Z, BOIKO V, MARKOWSKA M, *et al*. Optical studies of $Y_3(Al,Ga)_5O_{12}$:Ce^{3+},Cr^{3+},Nd^{3+} nano-phosphors obtained by the Pechini method. *Journal of Rare Earths*, 2019, **37(11):** 1132.

[33] XIA Z G, MEIJERINK A. Ce^{3+}-doped garnet phosphors: composition modification, luminescence properties and applications. *Chemical Society Reviews*, 2017, **46(1):** 275.
[34] WEI Z Y, MENG G H, CHEN L, *et al*. Progress in ceramic materials and structure design toward advanced thermal barrier coatings. *Journal of Advanced Ceramics*, 2022, **11(7):** 985.
[35] UEDA J, KUROISHI K, TANABE S. Yellow persistent luminescence in Ce^{3+}-Cr^{3+}-codoped gadolinium aluminum gallium garnet transparent ceramics after blue-light excitation. *Applied Physics Express*, 2014, **7(6):** 062201.
[36] MÉVEL C, CARREAUD J, DELAIZIR G, *et al*. First $ZnGa_2O_4$ transparent ceramics. *Journal of the European Ceramic Society*, 2021, **41(9):** 4934.
[37] KARACAOGLU E, ÖZTÜRK E, UYANER M, *et al*. Atomic layer deposition (ALD) of nanoscale coatings on $SrAl_2O_4$-based phosphor powders to prevent aqueous degradation. *Journal of the American Ceramic Society*, 2020, **103(6):** 3706.
[38] XU J, UEDA J, TANABE S. Novel persistent phosphors of lanthanide-chromium co-doped yttrium aluminum gallium garnet: design concept with vacuum referred binding energy diagram. *Journal of Materials Chemistry C*, 2016, **4(20):** 4380.
[39] BOIKO V, DAI Z F, MARKOWSKA M, *et al*. Particle size-related limitations of persistent phosphors based on the doped $Y_3Al_2Ga_3O_{12}$ system. *Scientific Reports*, 2021, **11:** 141.
[40] KATAYAMA Y, VIANA B, GOURIER D, *et al*. Photostimulation induced persistent luminescence in $Y_3Al_2Ga_3O_{12}$:Cr^{3+}. *Optical Materials Express*, 2016, **6(4):** 1405.
[41] BOIKO V, ZELER J, MARKOWSKA M, *et al*. Persistent luminescence from $Y_3Al_2Ga_3O_{12}$ doped with Ce^{3+} and Cr^{3+} after X-ray and blue light irradiation. *Journal of Rare Earths*, 2019, **37(11):** 1200.
[42] XU J, UEDA J, KUROISHI K, *et al*. Fabrication of Ce^{3+}-Cr^{3+} co-doped yttrium aluminium gallium garnet transparent ceramic phosphors with super long persistent luminescence. *Scripta Materialia*, 2015, **102:** 47.
[43] CHEN R, LAWLESS J L, PAGONIS V. A model for explaining the concentration quenching of thermoluminescence. *Radiation Measurements*, 2011, **46(12):** 1380.
[44] CHEN B, WANG F. Combating concentration quenching in upconversion nanoparticles. *Accounts of Chemical Research*, 2020, **53(2):** 358.
[45] WANG Z J, MEIJERINK A. Concentration quenching in upconversion nanocrystals. *Journal of Physical Chemistry C*, 2018, **122(45):** 26298.
[46] PAN Z W, LU Y Y, LIU F. Sunlight-activated long-persistent luminescence in the near-infrared from Cr^{3+}-doped zinc gallogermanates. *Nature Materials*, 2011, **11:** 58.

Cr^{3+}掺杂浓度对 YAGG:Ce^{3+},Cr^{3+}发光陶瓷余辉性能的影响

李廷松[1,2], 王文丽[1,3], 刘 强[3], 王雁斌[1,2], 周真真[1,2], 胡 辰[1,2], 李 江[1,2]

(1. 中国科学院 上海硅酸盐研究所, 透明陶瓷研究中心, 上海 201899; 2. 中国科学院大学 材料科学与光电工程中心, 北京 100049; 3. 江苏大学 材料科学与工程学院, 镇江 212013)

摘 要: $Y_3Al_2Ga_3O_{12}$:Ce^{3+},Cr^{3+}(YAGG:Ce^{3+},Cr^{3+})作为长余辉发光材料, 具有初始发光强度高和余辉时间长的优点, 在长余辉发光材料应用中具有广阔的前景。目前, YAGG:Ce^{3+},Cr^{3+}粉体具有良好的余辉性能, 但陶瓷的余辉性能还有待进一步优化。本工作通过固相反应及空气预烧结、热等静压烧结(HIP)后处理和空气退火制备了不同 Cr^{3+}掺杂浓度的$(Y_{0.998}Ce_{0.002})_3(Al_{1-x}Cr_x)_2Ga_3O_{12}$陶瓷, 研究了 Cr^{3+}掺杂浓度对陶瓷的微观结构、光学性能和余辉性能的影响。结果表明, 随着 Cr^{3+}掺杂浓度从 0.025%增加到 0.2%(原子百分数), 预烧结陶瓷或 HIP 后处理陶瓷的微观结构没有明显变化, 但陶瓷的直线透过率逐渐增加, 余辉性能逐渐下降。其中, 掺杂了 0.025% Cr^{3+}的 YAGG:Ce^{3+},Cr^{3+}陶瓷经过空气预烧结结合 HIP 后处理和空气退火后, 具有超过 6055 mcd/m^2 的最强初始发光强度和 1030 min 的最长余辉时间。本工作通过优化 Cr^{3+}掺杂浓度和制备工艺, 使得 YAGG:Ce^{3+},Cr^{3+}陶瓷的长余辉发光(PersL)性能得到明显提升。

关 键 词: YAGG:Ce^{3+},Cr^{3+}陶瓷; Cr^{3+}掺杂浓度; 长余辉发光; 热等静压烧结; 空气退火

中图分类号: TQ174 **文献标志码:** A **文章编号:** 1000-324X(2025)09-1037-08